

Preparation of Homogeneous Gas/Solid Suspensions for Efficient Downflow Reactors

Reto T. Meili

MSE Meili - Multiphase Systems Engineering, Technoparkstr. 1, CH-8005 Zurich
Tel: ++41-1-440 55 00, Fax: ++41-1-440 55 04, reto.meili@msemeili.ch

1 Abstract

The operation of downflow reactors in which gas/solids reactions with residence times below 100 ms should efficiently be performed, require at their inlet a continuous and stable delivery of an homogenous gas/solids suspension with loadings in the range 0.5 to 3. In a test facility with a maximum solids throughput of 5 t/h a fluidised bed dosing system in conjunction with either a mixing tube containing an aerated 'lance' or a convergent-divergent nozzle were used for solids feeding and dispersion. To characterise the produced gas/solids suspension γ -absorption computer tomography was used to measure the local solids concentration and a fibre-optical probe was employed to simultaneously determine local particle concentration fluctuations and solids velocities.

The experiments proved that both systems investigated were able to produce an homogenous gas/solids dispersion - the mechanical insert 'lance' offering the capability to adjust the produced solids distribution from 'u-shaped' to homogeneously distributed and the convergent-divergent nozzle being a simple device in which the particles are dispersed by gas turbulence only.

2 Introduction

2.1 General

Mixtures of gas with finely grained solids with particle sizes below 100 μm are due to their high surface area very reactive. A vivid illustration of this reactivity is the dreadful power of dust explosions. Technical means to perform such a reaction continuously and in a controlled way are therefore of interest since they offer a high potential for savings of raw material, energy and costs [1]. At temperatures above 1'100 °C many reactions of industrial relevance are completed within residence times of 10 – 500 ms only. Therefore the main difficulty to overcome is to 'handle' the educt gas/solids feed in a controlled way ensuring

optimum reaction conditions for all reactants within time frames of milliseconds.

Reactions between gases and solids are commonly used within the processing industries. Roughly they may be divided into *catalytic* and *non-catalytic* gas/solids reactions with oxidation & reduction, (de-) hydration, isomerisation and cracking being the most important basic reactions. Doraiswamy and Sharma compiled over 80 reactions of industrial relevance /2/. Figure 2-1 shows as an example the kinetic data of the fast degasification of an high volatile bituminous (hvb) coal /3/.

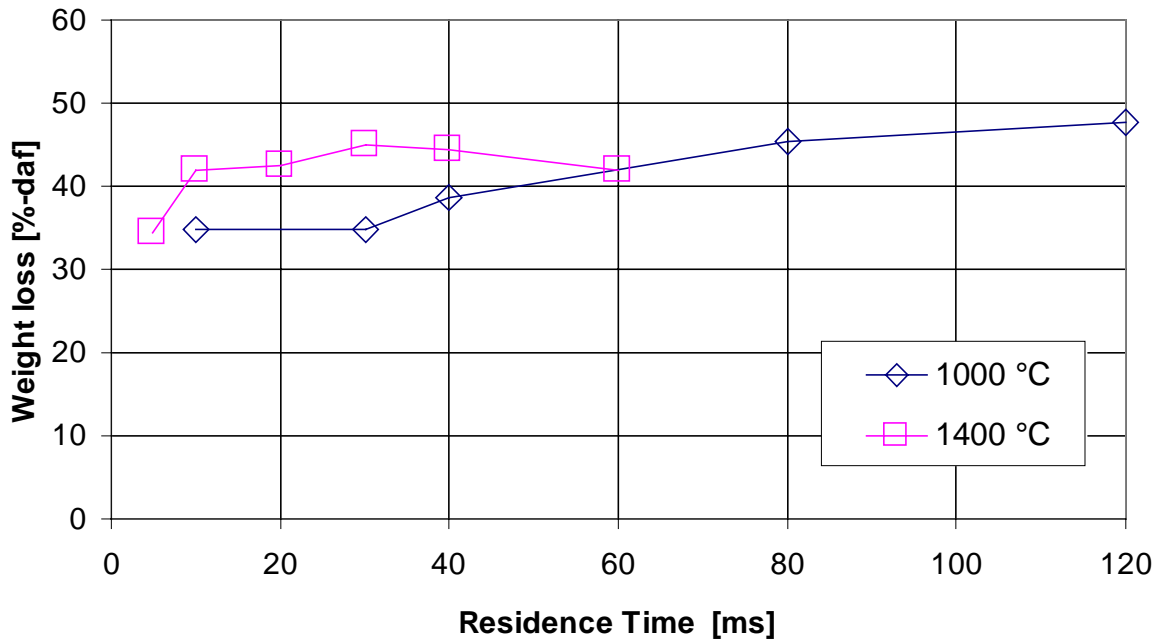


Fig. 2-1: Weight loss as a function of residence time at the degasification of coal particles $< 75 \mu\text{m}$ ($d_{p50,3} = 32 \mu\text{m}$, daf: 'dry ash free', /3/).

2.2 Downflow Tube Reactor

To provide the optimum reaction conditions for all reactants evenly *constant temperatures* together with *narrow residence time distributions* are to be demanded. A downflow tube reactor ('downer') continuously operated and fed with educts in an optimum mass flow ratio would fulfil these demands. To achieve a defined reaction stop means for either quenching or rapid separation of the products from the gas have to follow the reactor tube. The latter may be realised using a cyclone operating efficiently at high loadings.

Since residence times below one second would not allow much time to compensate greater concentration inhomogeneties in the reactor, *an homogeneous gas/solids suspension* has to be prepared *outside the reactor* and *fed as fluctuation free as possible* into the reactor. This suspension should have the optimal loading for the particular reaction.

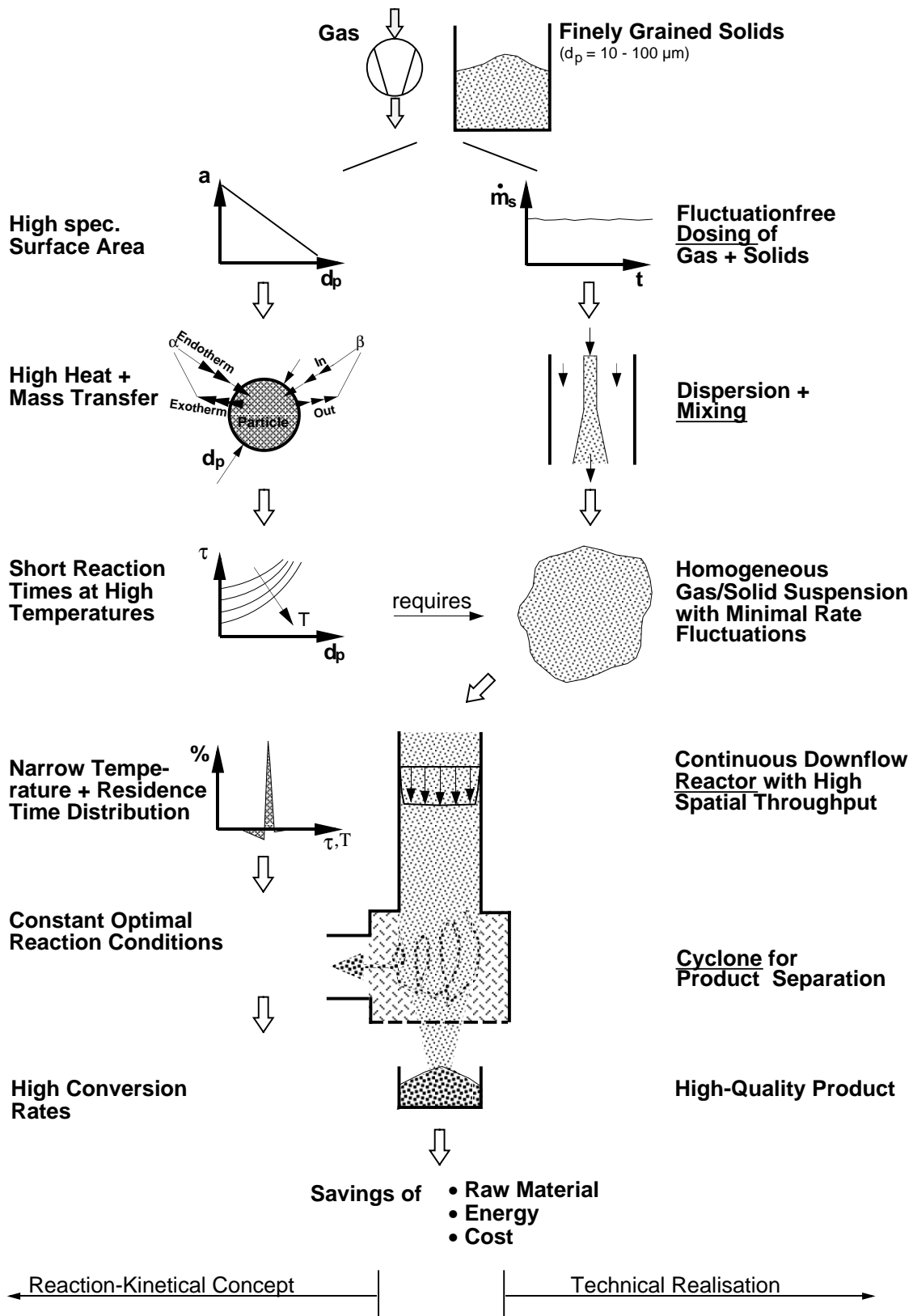


Fig. 2-2: Concept of a fast downflow tube reactor with the unit operations of 'dosing', 'mixing', 'reacting' and 'separation.'

In the herein pursued concept the solids are time-constantly dosed in a first step and in a second step dispersed and mixed with air in order to produce an homogeneous gas/solids suspension with a loading in the technical relevant range

of $\dot{\mu} = \dot{m}_s / \dot{m}_g = 0.5 - 3$. Figure 2-2 gives an overview over this concept including the most important causal dependencies.

Process	Reaction	Particle-size [μm]	Temperature [$^{\circ}\text{C}$]	Residence-time [ms]	Loading [-]	Status	References
Smelting of Cu/Sn/Zn-concentrates	Ox, Red	10-200	1050-1600	< 1000	0.5-0.8	Demo	/9, 15, 33, 44, 45/
Melting of dust residues	Ox, Red		1600-1700	100-500		Industrial (up to 3 t/h)	/10-12/
Contaminated soils treatment	Ox, Red	45-1180	1400-1800				/16/
Mineralization of sewage sludge	Ox		1400-1500			Pilot	/43/
Waste-Gasification (Noell)	Ox, Red					Industrial (30 t/h)	/28, 29/
Pyrolysis of biomass	Pyrolysis		850	70		Pilot	/5/
Pressurised coal gasification (Prenflo, Shell)	Pyrolysis	< 100	> 2000	10-100		Demo (2 t/h)	/14, 18- 21/
Coal combustion	Ox	< 200	700-1800	10-3000	0.1-0.5	Laboratory	/22-27/
Dry desulphurization	Ox, Red	1-10	700-1400	10-300	0.07	Laboratory (~1 g/min)	/4, 30-32/
Calcination	KSZ	1-10	700-1400	10-300	0.07	Laboratory (~1 g/min)	/4, 30-32/
Oil cracking	FCC	60/210	600-900	150-500	~ 1	Pilot	/17/
Glass melting	Ox					Demo (15 t/d)	/34/
Metallurgical plasma reactors	Plasma	2-80, 0.005-0.05	2000-18000 (arc)	~ 100	0.5-1.1	Pilot	/35-38, 42, 46/
Recrystallisation of ferrite powders	Neutr	50-500	700-1600	< 3000		Pilot	/39/
Metallurgical high temperature synthesis of TiC	Neutr	2-75	1500-3000		0.5-2	Laboratory	/47/
Storage of solar H ₂ with metal oxides	Red	0.1 - 1	1000-2300	~ 100		Pilot	/40, 41/
Legend	Ox oxidating atmosphere Neutr neutral atmosphere			Red reducing atmosphere FCC fluid catalytic cracking			

Table 2-1: Overview of 'fast' gas/solid reactions and their development stage.

Within other research groups similar concepts for fast gas/solids processing are pursued, i.e. Fan /4/ or Bergougnou /5/, confirming the low achievable reaction

times below 100 ms. Table 2-1 gives an overview over application areas of fast gas/solids reactors and their development stage.

2.3 Short-time constant Dosing

The herein used dosing techniques were developed in a preceding project and described in detail by Tesch in /6/, therefore a short outline of the technique should be given at this point only. Figure 2-3 shows the principle: a stationary fluidised bed is operated slightly above minimum fluidisation. Through a specially designed, cylindrical nozzle the solids discharge continuously like a 'fluid' at a very even flow rate provided that there are no pressure fluctuations and the bed high H_{WS} is held constant. This is achieved using a controlled screw feeder. According to Tesch /6/ the discharging solids mass flow comes to:

$$\dot{m}_{s,0} = \rho_s \cdot (1 - \epsilon_{WS}) \cdot A_A \cdot \sqrt{g \cdot (H_{WS} + L_A)} \quad (2.1)$$

for $d_A \geq 0.020$ m.

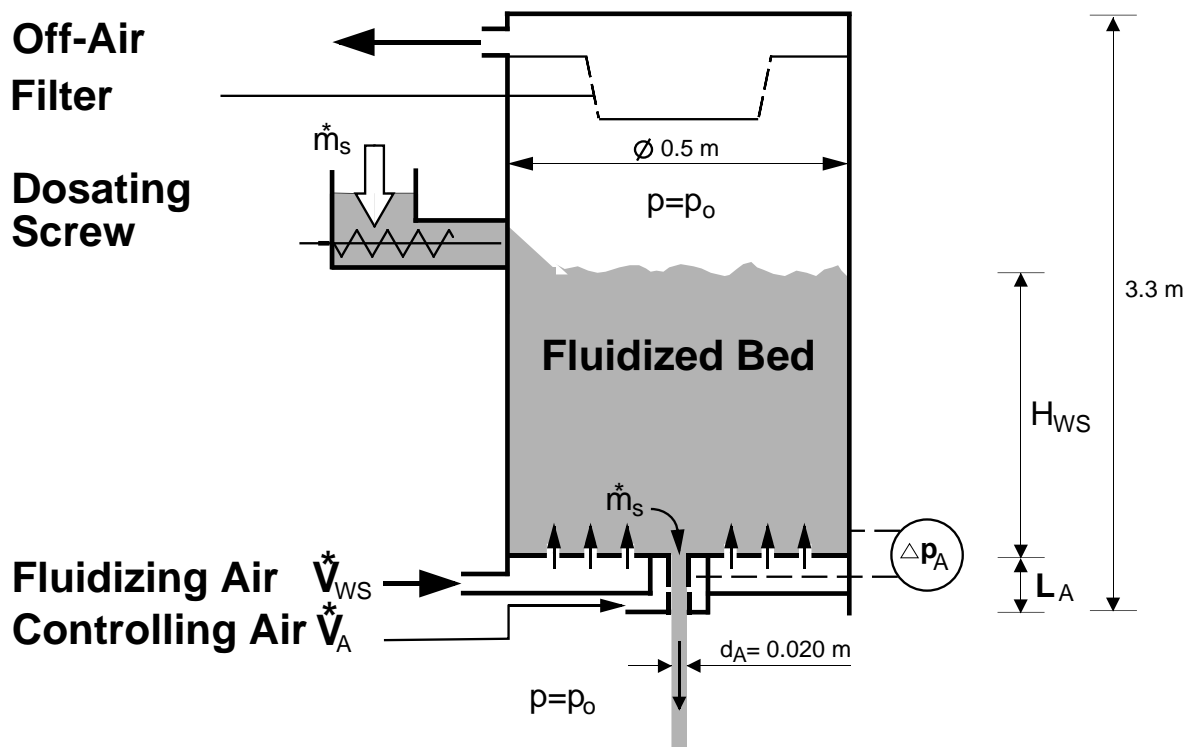


Fig. 2-3: Principle of short-time constant dosing out of stationary fluidised bed.

For the fast determination of the discharging mass flow rate Tesch established the following relation between the 'driving' pressure difference Δp_A measured at the bottom of the fluidised bed and a certain point in the discharging nozzle and the solids mass flow rate:

$$\dot{m}_{s,A} = A_A \cdot \sqrt{\rho_{WS} \cdot \Delta p_A + \frac{\rho_{WS}^2 \cdot V_A \cdot g}{A_A}} \quad (2.2)$$

V_A represents the balance volume of the eq. 2.2 underlying momentum balance and needs to be determined experimentally. Advantages of this measuring method are besides its simplicity the high achievable measuring rate of more than 100 Hz.

Figure 2-4 presents exemplary measuring results obtained according to eq. 2.2: The time series for mono-disperse glass beads as well as the one for fluid cracking catalyst (FCC) show so far unprecedented low dosing fluctuations with variation coefficients¹ as low as 0.04% and 0.15% respectively.

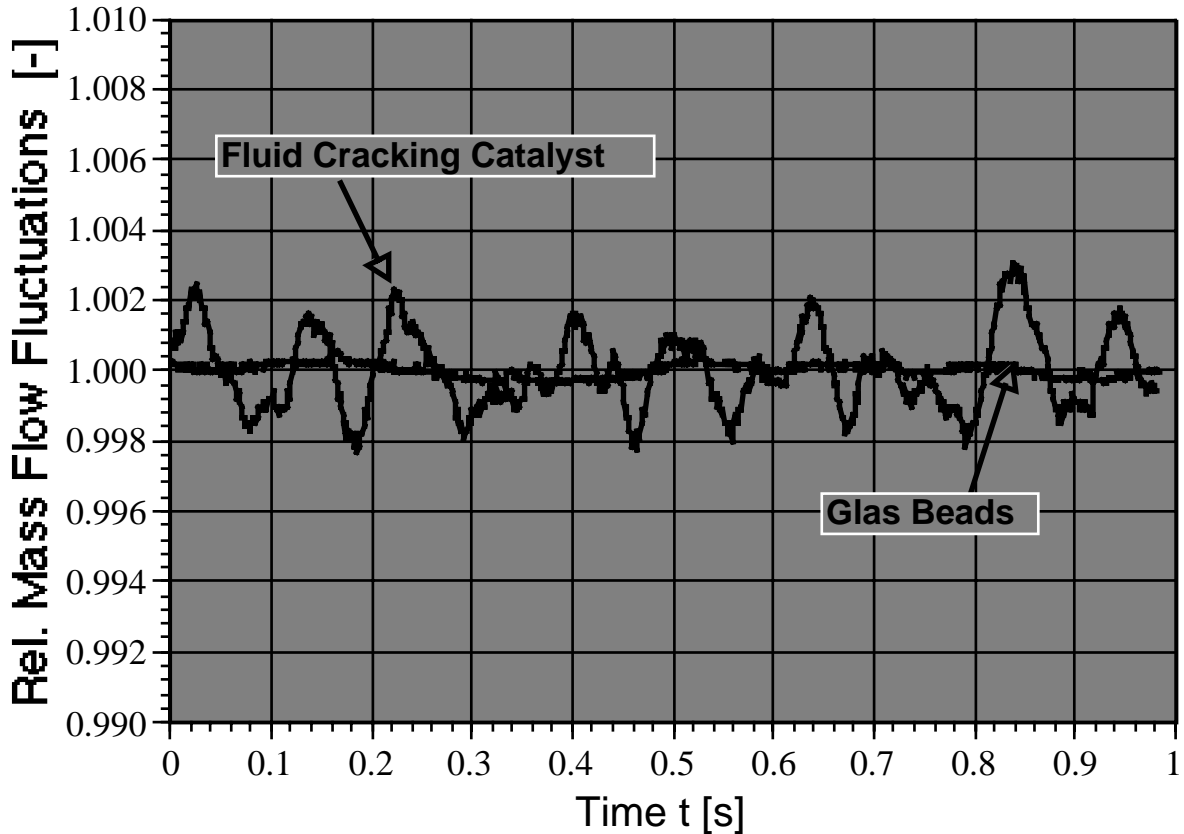


Fig. 2-4: Mass flow rate time series for mono-disperse glass beads ($d_{p50,32} = 74 \mu\text{m}$) and fluid cracking catalyst FCC ($d_{p50,32} = 59 \mu\text{m}$, $d_A = 20 \text{ mm}$, $L_A = 107 \text{ mm}$, $H_{WS} = 0.73 \text{ m}$, $\dot{m}_s \approx 5 \text{ t/h}$, /6/).

3 Experimental Techniques

3.1 Test Unit & Materials

The experiments were carried out using the semi-technical test unit shown in figure 3.1 with a continuous solids through-put of up to 5 t/h. The installation comprises the fluidised bed feeder described in the preceding chapter, a mixing zone where different mixing units could be mounted and all the necessary infra-

¹ Standard deviation divided by arithmetic mean.

In the mixing zone the solids are dispersed and mixed with up to 6500 m³/h of air from two roots blowers. After the mixing section the solids were separated from the air by means of a combined cyclone / bag-filter and from there conveyed via a fluidised 'u-seal' by means of a bucket elevator back to the solids bin. The use of a bucket elevator prevents classification and also attrition of the solids. For calibration purposes according to eq. (2.2) the solids could be directed to a scale after the mixing zone, where the mass flow rate was measured.

To achieve operating conditions as stable and fluctuation-free as possible all pressure fluctuations - especially the ones over the fluidised bed - have to be minimised. In order to do so various measures were taken as i. e. the filter above the fluidised bed is dedusted continuously without blasts, the feeding and mixing section are decoupled from the rest of the unit as the pressure levels correspond to atmosphere and 'laval-nozzles' or roots blowers with steep characteristics were used for the air supply.

All experiments were carried out under *ambient conditions using air and glass beads* as test materials. The glass beads particle size distribution was nearly mono-disperse with a solids density of $\rho_s = 2560 \text{ kg/m}^3$ and a mean diameter of $d_{p50,3} = 66 \text{ }\mu\text{m}$.

3.2 Measuring Techniques

To characterise the produced gas/solids suspension completely a measuring concept was pursued that distinguishes between the *stationary* and the *dynamic characterisation*. So all relevant parameters of the test unit as indicated in figure 3.1 as well as the local solids distribution were measured as time averaged values, while a system for laser-backscatter photometry with fibre-optical probes was used for the dynamic characterisation of the gas/solids suspension.

Figure 3.2 presents a schematic of the arrangement for **γ -absorption-computer tomography** used to determine the local solids distribution measuring the absorption I/I_0 of a collimated γ -ray. The relation between absorption I/I_0 and local solids volume fraction $1-\epsilon_i$ is given by Lambert-Beers law in discrete form:

$$\frac{I}{I_0} = e^{-\sum_i D_{\text{obs},i} \cdot \Delta l_i} \quad (3.1)$$

with
$$D_{\text{obs},i} = (1-\epsilon_i) \cdot (D_s - D_g) \quad (3.2)$$

the local 'observed' absorption coefficients.

D_s and D_g are the linear absorption coefficients of glass beads and air respectively. With the used Iod¹²⁵ source emitting radiation with an energy of 35 keV D_g being about 4 orders of magnitude smaller than D_s is neglectable. D_s is determined experimentally using 6 glass tiles of different thickness, which were made by melting the used glass beads and equals $D_s = 305.4 \text{ 1/m}$.

Equation (3.2) solved for $(1-\varepsilon_i)$ yields the solids volume fraction as a function of $D_{\text{obs},i}$ and D_s :

$$1-\varepsilon_i = D_{\text{obs},i} \cdot D_s \quad (3.3)$$

The $D_{\text{obs},i}$ in equation (3.3) were determined by numerical reconstruction ('computer tomography') of absorption values I/I_0 measured at 256 positions assuming rotational symmetry - for a detailed description of the measuring techniques please cf. /7/.

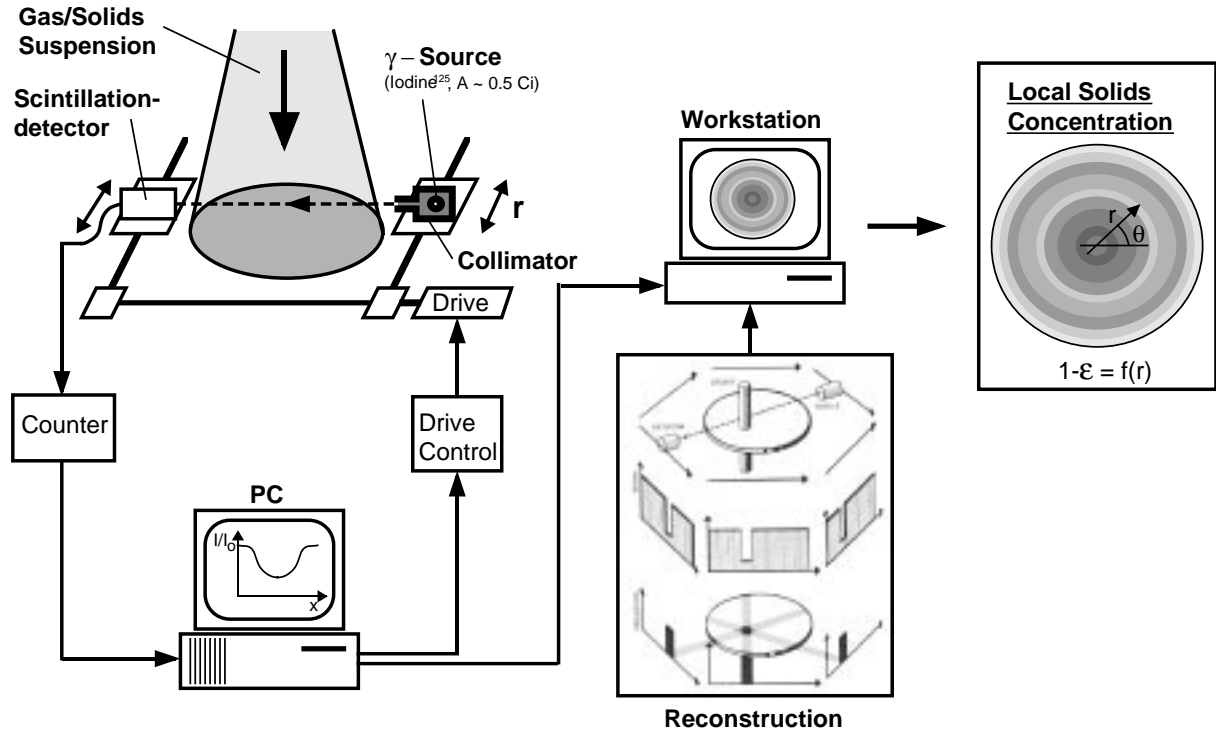


Fig. 3.2: Principle of γ -absorption-computer tomography.

The arrangement for **laser-backscatter photometry** used² is shown in figure 3.3. By means of optical fibres laser light is brought into the gas/solids suspension, which is backscattered partially by the solids, received by additional fibres and converted into a voltage signal. The intensity of this signal corresponds to the solids volume fraction in front of the probes. Using two probes at a distance of Δd in flow direction, the local solids velocity c can be determined correlating the two - time shifted - signals calculating the 'time of flight' τ^* /7,8/. - In this work this system is used for the characterisation of the dynamic behaviour of the gas/solids suspension as well as for solids velocity measurements only, whereas the quantitative concentration data is determined by γ -absorption-computer tomography.

² The arrangement in figure 3.3 represents a configuration as used for the experiments described herein - at present time much more advanced arrangements are available.

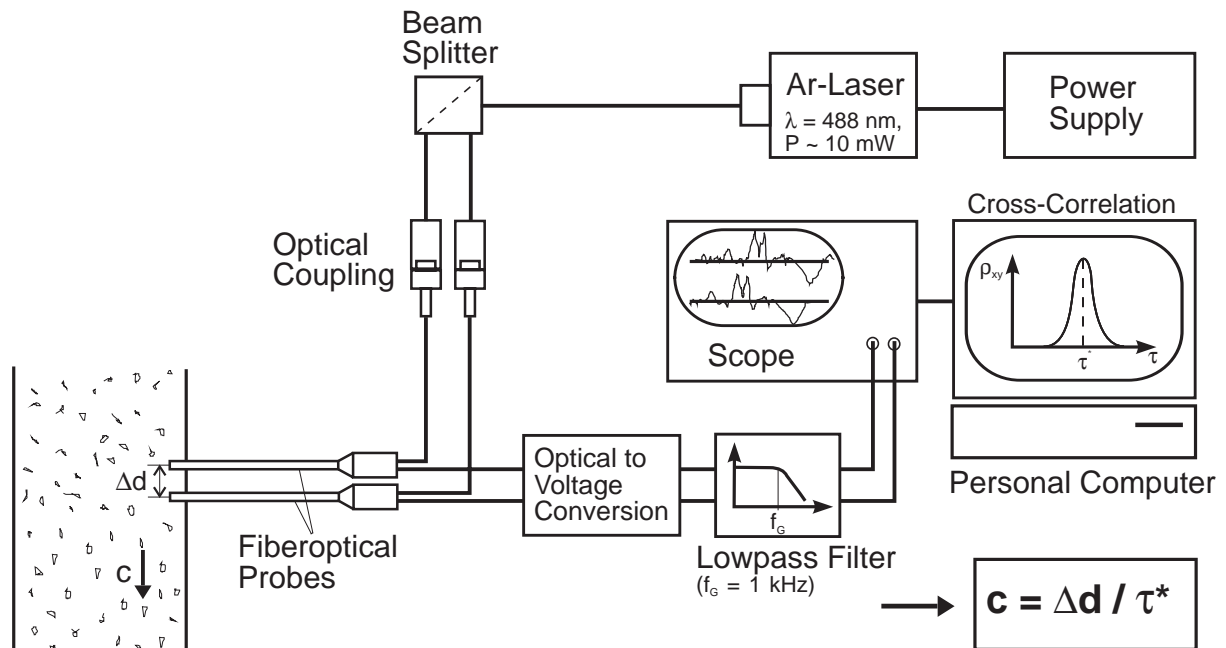


Fig. 3.3: Laser backscatter-photometry system for the solids velocity determination and fluctuation characterisation.

4 Dispersion - Results

4.1 Dispersion Principles

The fluidised bed dosing system as described in chapter 2.3 delivers a stable, highly loaded ($\dot{\mu} \cong 2500$ kg solids per kg of gas) gas/solids stream, which exits the fluidised bed with a downward velocity of ca. 4 m/s being accelerated in ambient atmosphere like in vacuum due to air friction unmeasurably low /6/. To produce out of this compact gas/solids stream an homogenous suspension with a target loading $\dot{\mu}$ in the range of 0.5 to 3³, the solids needs to be dispersed. This means to overcome the significant inertia of the spatially highly concentrated solids. Since modelling of such highly loaded suspensions with the pretension to actually predict the behaviour of the gas/solids flow is not possible, an experimental approach is required.

Preliminary experiments with different nozzles / tube configurations lead to two promising solution variants: In a first the solids are dispersed by means of mechanical insert, which allows the direct injection of air in the core of the solids stream. In a second approach the solids were 'detached' from the core stream in the boundary layer of a fast flowing turbulent gas flow. Both variants have been realised - the concrete experimental set-up together with the achieved dispersion results are presented in the following.

³ This equals a solids volume fraction 1-ε of 0.025% to 0.15% for glass beads and neglected relative velocity.

4.2 Mechanical Dispersion - 'Lance'

Figure 4.1 shows the set-up to mechanically disperse the gas/solids stream: A sharp 'lance' is positioned by three adjustable wires in the centre of the down flowing solids. Through a hose air emitted radially from the lance tip $\dot{m}_{g,L}$ was supplied. The addition of a minor amount of 'stabilising air' kept the gas/solids stream stable from the exit of the fluidised bed through the gas distributor into to mixing tube. Through a gas distributor the mixing air \dot{m}_g was distributed equally over the radius of the mixing tube.

Figure 4.2 shows the by γ -absorption-computer tomography measured radial *solids distributions* for two different solid mass flow rates, two different mixing tube lengths (left and right columns) and three different lance aeration levels (top down). With no air emitted through the lance, the solids are just deviated by the steep lance tip forming a dense, free-falling particle curtain (ordinate not similar scaled than other graphs!). Emitting air through the lance this curtain can be widened up producing quite homogenous solid distributions at the end of the longer mixing tube. If too much air is emitted the solids are collected at the tube wall.

The *solids velocities* measured for the medium lance aeration level are presented in figure 4.3. Measurements at different axial positions have different symbol *form*, the two mass flow rates are characterised by *filled and empty* symbols. The velocity profiles are similar to single phase flow profiles - in the centre higher and at the wall lower than the superficial gas velocity of $u_0 = 5.4$ m/s. At higher solids mass flow rates the profiles look qualitatively the same but are 1 to 2 m/s higher. The fact, that all solids velocities measured are within a difference of less than 2 m/s to the superficial gas velocity corresponds well to the measured low concentration profiles - the *gas phase seems to dominate the flow structure*.

The ability to produce continuously falling particle curtains found a first technical application in the moistening of fly-ash of thermal power plants as water is sprayed directly to the free accessible surface of the ash - a very direct process route without moving parts /13/.

4.3 Convergent-Divergent Nozzle

To disperse the solids fluid-dynamically a convergent-divergent nozzle as shown in figure 4.4 was used. In a convergent inlet zone the gas is accelerated and brought in contact with the solids. In the following narrow mixing tube the dense solids stream is dispersed in the boundary layer of the turbulent gas flow. In the mixing tube superficial gas velocities u_0 in the range of 35 up to 80 m/s were adjusted. Particles that are once detached from the compact stream and dispersed are very rapidly accelerated by the gas causing an high pressure drop.

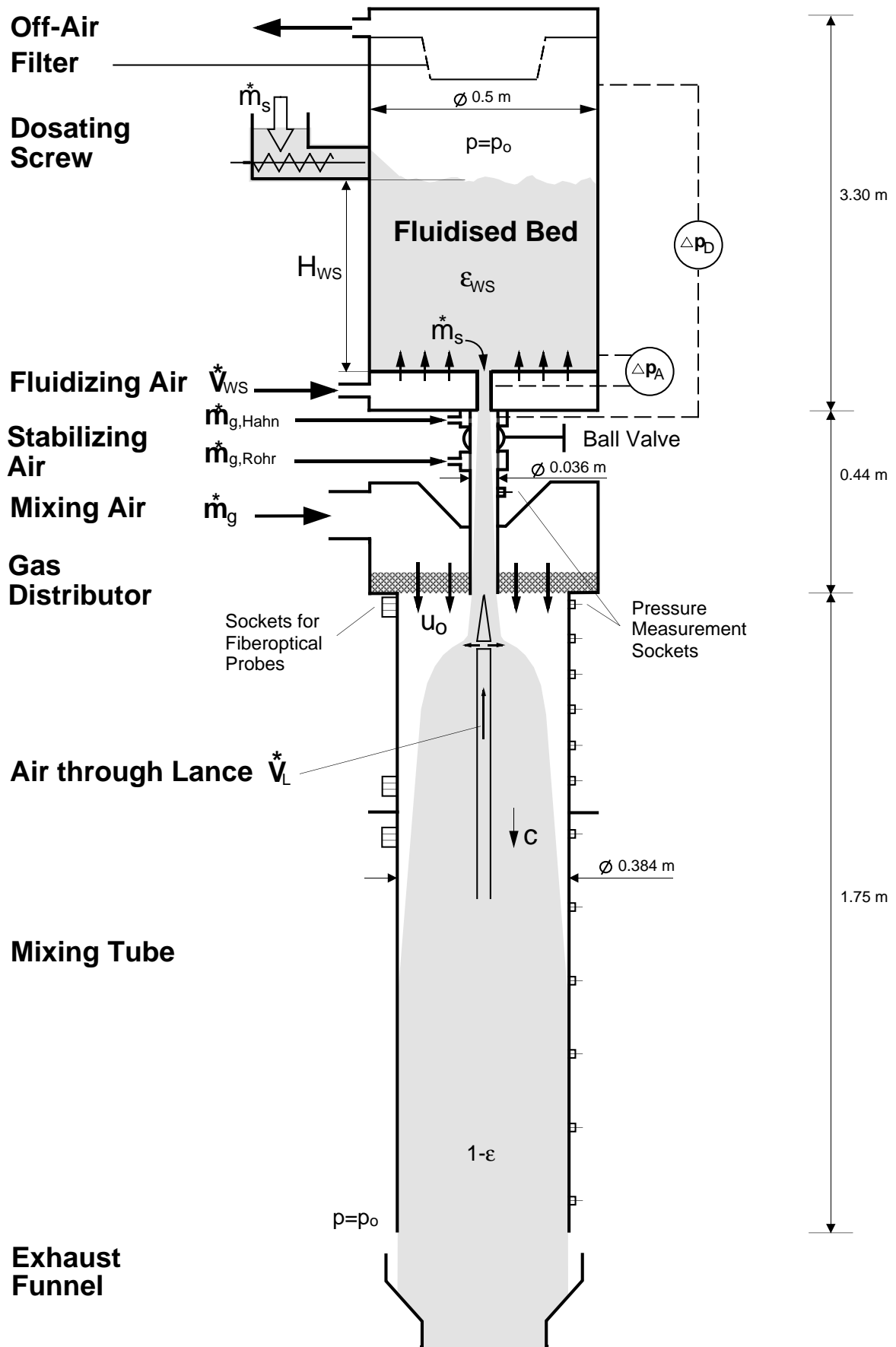
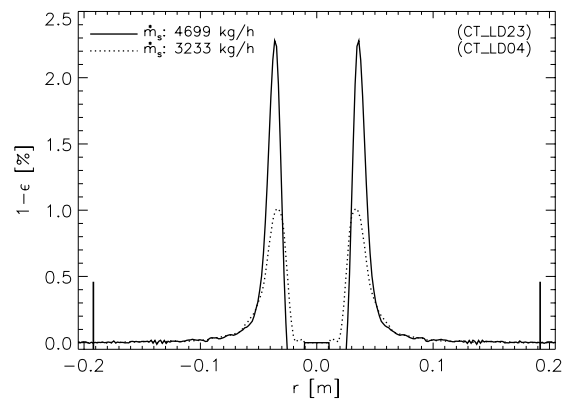
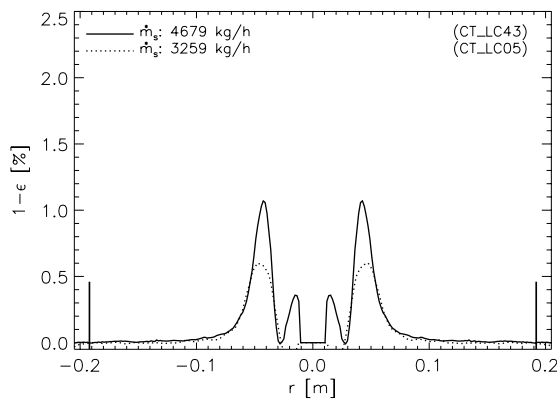
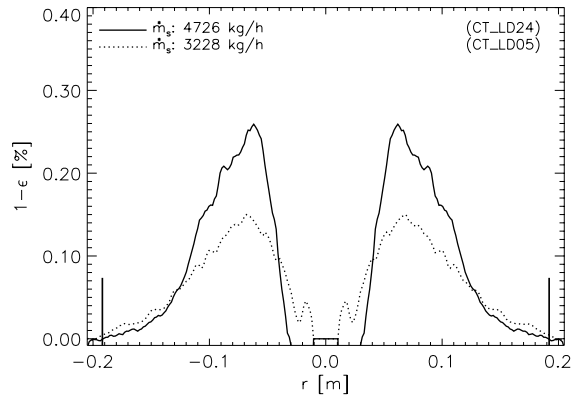
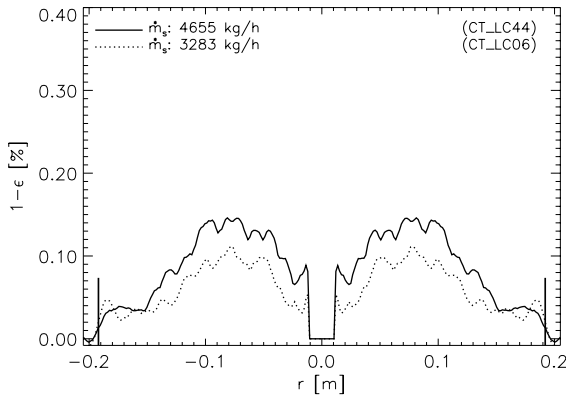


Fig. 4.1: Experimental configuration 'lance': a sharp lance emitting air radially disperses the solids stream from the inside.

$$\dot{m}_{g,L} = 0 \text{ kg/h}$$



$$\dot{m}_{g,L} = 28.1 \text{ kg/h}$$



$$\dot{m}_{g,L} = 47.5 \text{ kg/h}$$

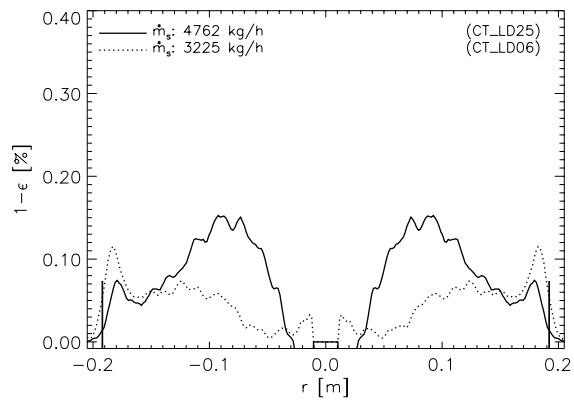
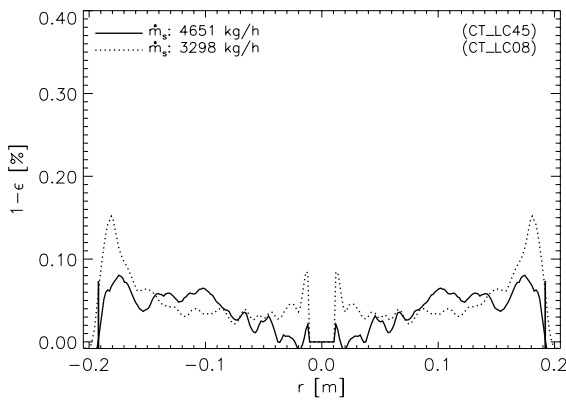


Fig. 4.2: Radial solids volume distributions 'lance' for two different solids flow rates \dot{m}_s and tree different lance air flows $\dot{m}_{g,L}$ ($\dot{m}_g = 2.49 \text{ t/h}$, $u_0 = 5.4 \text{ m/s}$).

Left: Tube length = 1.752 m (LC) **Right:** Tube length = 1.128 m (LD)

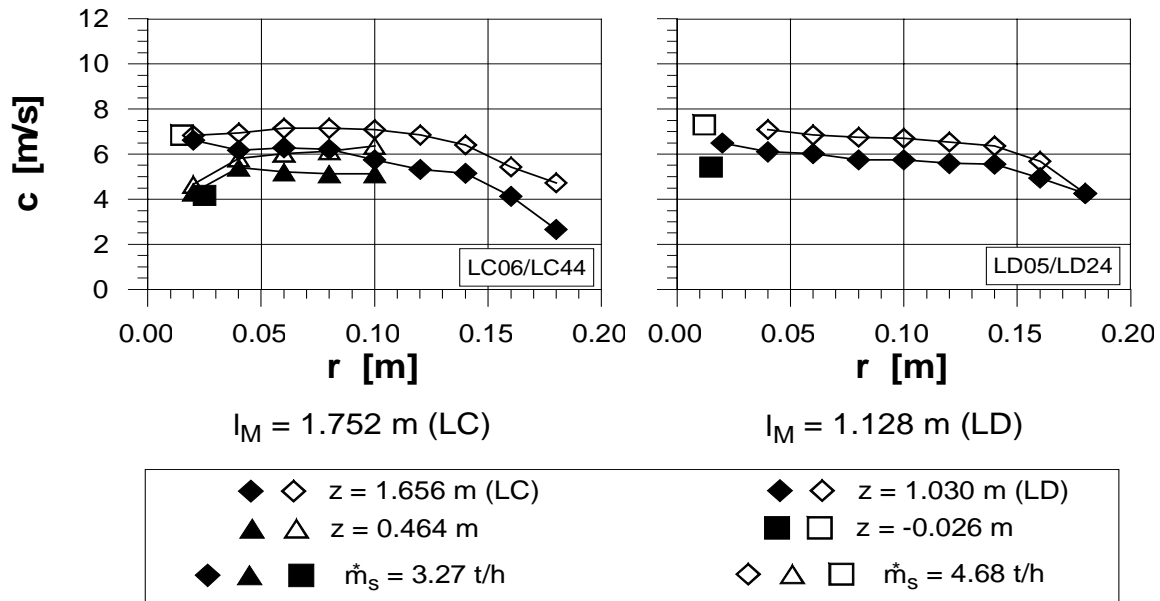


Fig. 4.3: *Radial solids velocity profiles 'lance' at different axial positions z and for two different tube lengths ($\dot{m}_{g,L} = 28.1 \text{ kg/h}$, tube diameter $d_M = 0.384 \text{ m}$, $\dot{m}_g = 2.49 \text{ t/h}$, $u_0 = 5.4 \text{ m/s}$).*

The narrow diffuser that follows the mixing tube recovers up to 80% of this pressure drop and at the same time enhances the homogeneity of the solids distribution offering additional 'time' or 'length' for settling processes.

Figure 4.5 shows at the end of the diffuser measured radial *solids concentrations* of experiments at three different solids mass flow rates. At a superficial gas velocity of 35.5 m/s the degree of turbulence is not high enough to disperse the solids stream: in this 'subcritical' condition the gas/solids stream is at the end of the diffuser still fairly compact - as shown in the top graph of figure 4.5.

As the gas throughput is enhanced the solids are first partially and then quite homogeneously dispersed - the lower the solids mass flow rate the better.

Measured *solids velocity distribution* at the end of the diffuser is represented in figure 4.6: solids velocities of more than 40 m/s at a superficial gas velocity of 21.7 m/s show, that the phases are not balanced yet. The deviations from rotational symmetry in figure 4.6 are caused by the non ideal one sided gas inlet - enhancements at this point are indicated.

Investigations of the *solids fluctuations* in the convergent-divergent nozzle analysed by different statistical sizes, yielded *high fluctuations* especially at the beginning of the mixing tube and in regions of the nozzle, where the particles were *incompletely dispersed*. Since the fluctuations are much lower in regions, where the solids were well dispersed, the conclusion is drawn, that well *dispersed solids dampen the turbulence of the gas* (for more details cf. /7/).

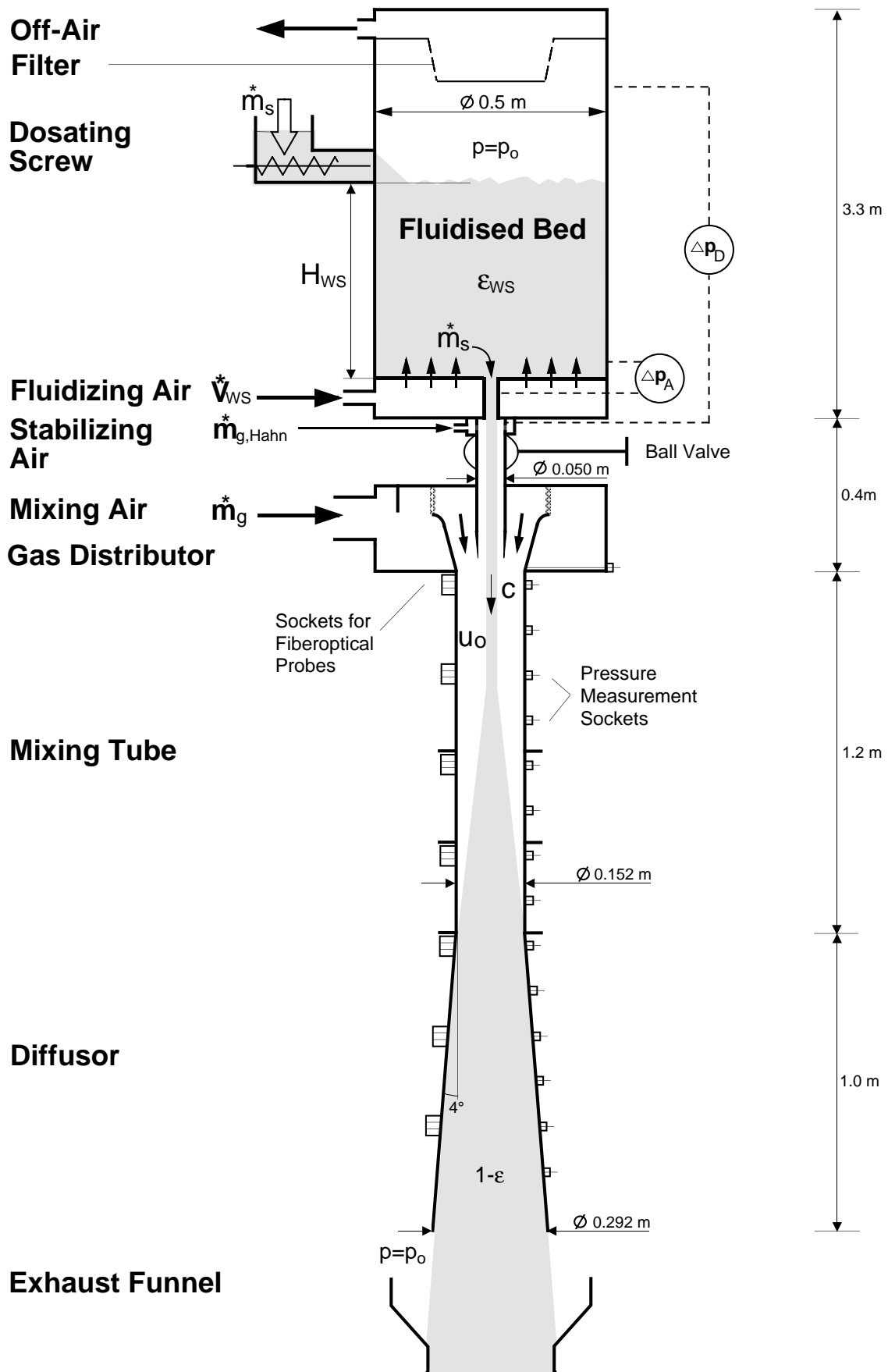
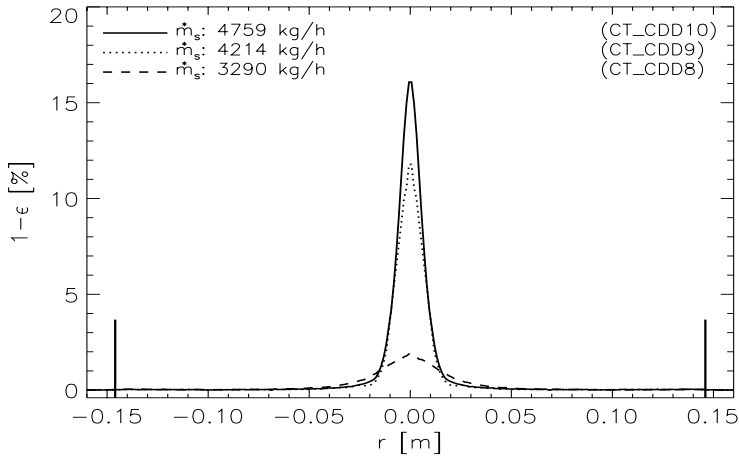
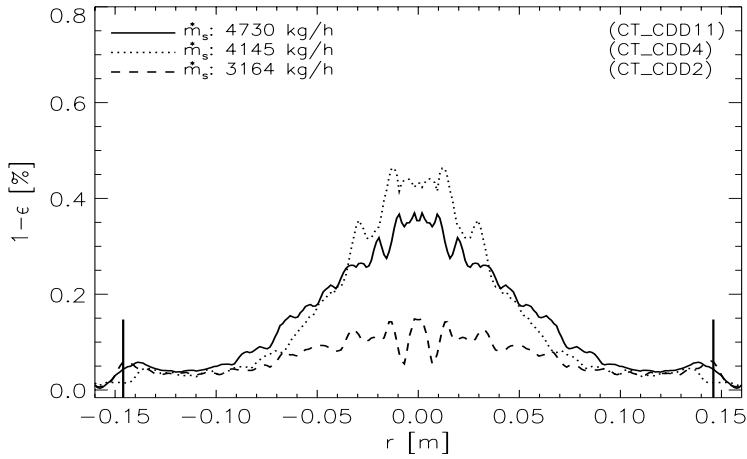


Fig. 4.4: Experimental configuration 'convergent-divergent' nozzle: the solids are dispersed in the turbulent gas flow of the mixing tube.

$\dot{m}_g = 2.52 \text{ t/h}, u_0 = 35.5 \text{ m/s} (u_{\text{Diff}} = 9.6 \text{ m/s})$



$\dot{m}_g = 3.53 \text{ t/h}, u_0 = 52.4 \text{ m/s} (u_{\text{Diff}} = 14.2 \text{ m/s})$



$\dot{m}_g = 4.47 \text{ t/h}, u_0 = 64.9 \text{ m/s} (u_{\text{Diff}} = 17.6 \text{ m/s})$

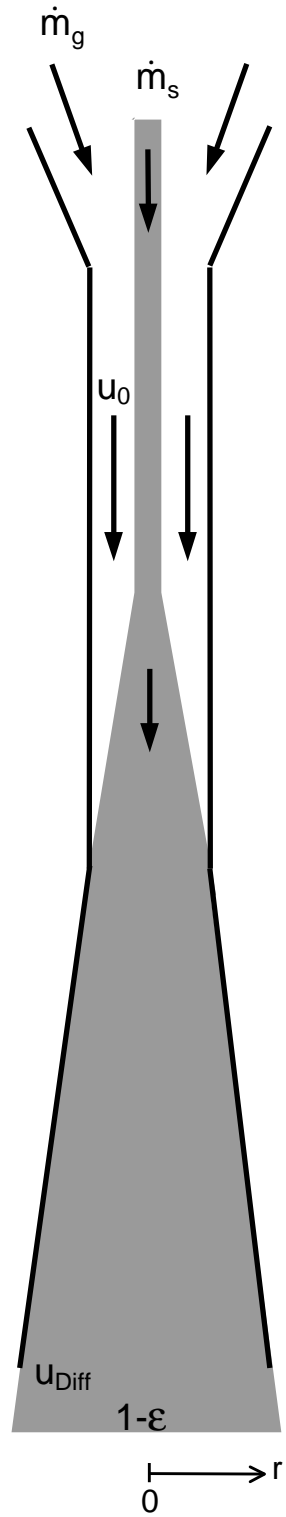
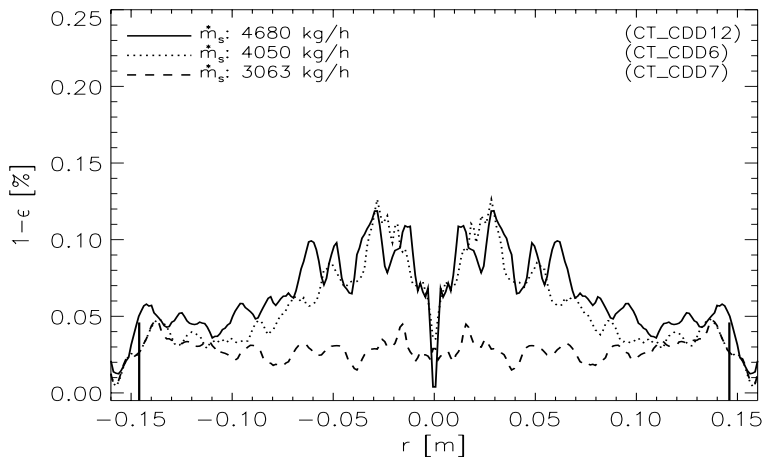


Fig. 4.5: Radial volumetric solids distribution profiles in the convergent-divergent nozzle (different scaling of the ordinates!).

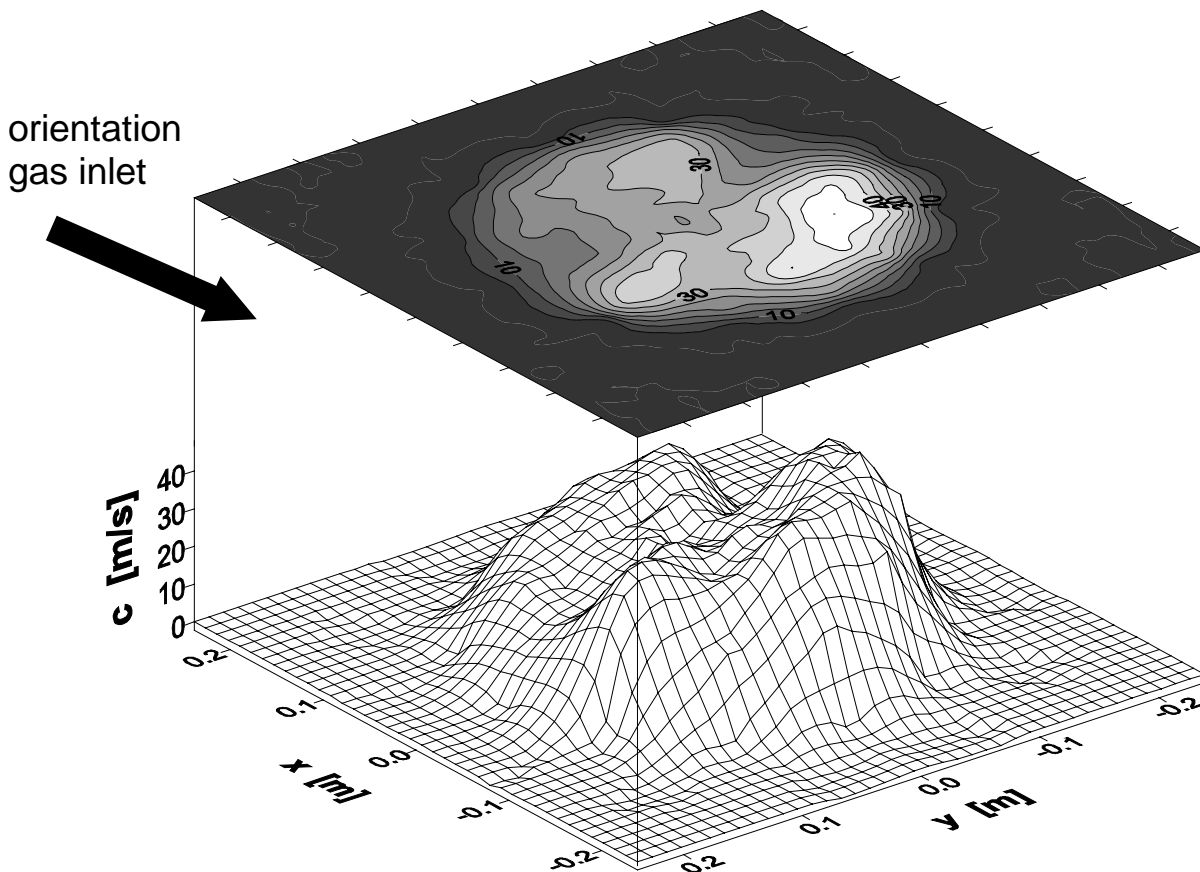


Fig. 4.6: Local time averaged solids velocities at the end of the diffuser (run 'CDD3/20', $z = 2.234$ m, $\dot{\mu} = 0.59$, $u_{\text{Diff}} = 21.7$ m/s).

5 Conclusions

The two different concepts investigated to disperse a dense gas/solids stream were both suited to produce an homogenous gas/solids suspension. The dispersion with mechanical inlets as the used aerated 'lance' has the advantage, that the solids distribution profile may be varied from 'u-shaped' to *homogenous independently from the solids loading*. The dispersion in a convergent-divergent nozzle requires an high degree of turbulence and therefore *high gas velocities* in the mixing tube for a complete solids dispersion, what restricts the target loading to values lower than $\dot{\mu} \leq 1.0$. - Even if not all questions are finally resolved, it was shown, that homogenous gas/solids suspensions as claimed in the introduction to be necessary for the efficient operation of fast fast/gas solids reactors can be produced by different set-ups - so that from this side no major technical obstacles are in the way to the application of such reactors.

6 Acknowledgements

This work was supported by the 'Kommission für Technologie und Innovation' (KTI) of the Swiss government and by Buhler Ltd., Uzwil Switzerland - the author like to thank for their continued financial support.

7 Notation

A	area	m^2	Δp_A	pressure difference between	
A_γ	activity γ -source	Bq		bottom of the fluidised bed and	
c	solids velocity	m/s		drilling in discharge nozzle	Pa
d	diameter	m	r	radius, co-ordinate	m
d_p	particle diameter	m, μm	t	time	s
$D_{obs,i}$	observed linear absorption coefficient	1/m	u_0	superficial gas velocity	m/s
D_i	linear absorption coefficient	1/m	u_{Diff}	superficial gas velocity at diffuser exit	m/s
Δd_{opt}	gap between fibre-optical tips	m, mm	V_A	volume of discharging area	m^3
H_{WS}	height of fluidised bed	m	\dot{V}_g	gas flow rate	m^3/s
ϵ	porosity (void fraction)	-	z	co-ordinate	m
ϵ_{WS}	porosity fluidised bed	-	$\dot{\mu}$	loading: \dot{m}_s / \dot{m}_g	-
$1-\epsilon$	solids volume fraction,		ρ	density	kg/m^3
	$(1-\epsilon) 100 = (1-\epsilon)\%$	-, %	$\rho_{xy}(t)$	cross-correlation coefficient	-
I	transmitted radiation intensity	Bq	Indices		
I_0	radiation intensity measured through air	Bq	A	discharge ('Auslauf')	
l	length (of radiation path)	m	g	gas	
Δl	step length γ -abs.-CT	m	L	lance	
L_A	length discharge nozzle	m	M	mixing tube	
\dot{m}_s	solids mass flow rate	kg/s	p	particle	
$\dot{m}_{s,0}$	solids mass flow rate eq. (2.1)	kg/s	s	solids	
$\dot{m}_{s,A}$	solids mass flow rate discharging from fluidised bed, eq. (2.2)	kg/s	WS	fluidised bed ('Wirbelschicht')	
\dot{m}_g	gas mass flow rate	kg/s	0	ambient condition, number	
$\dot{m}_{g,L}$	gas mass flow through lance	kg/s	1	length	
p	pressure	Pa	2	area	
Δp	pressure difference	Pa	3	volume, mass	

8 References

- /1/ REH, L.: Verfahrenstechnik feinkörniger Feststoffe bei hohen Temperaturen - Stand und Möglichkeiten, *SwissChem* 10 (1988), Nr. 3, S. 21-42
- /2/ DORAISWAMY, L. K.; SHARMA, M. M.: Heterogeneous Reactions: Analysis, Examples and Reactor Design, *Volume 1 Gas-Solid and Solid-Solid Reactions*, John Wiley & Sons, New York, 1984

- /3/ HAAS, J.H.P., LOCKEMANN, S.A. et al.: Combustion characterisation for a suite of different coals, Ijmuiden, International Flame reasearch Froundation (IFRF), IFRF Doc. No. F37/y/35 (1995)
- /4/ FAN, L. S.; RATHMAN, J.; DASTIDAR, A. G.; WEIMER, A. W.; KIMURA, S.: The Potential of Reaction Engineering, *Chemical Engineering Progress* (1994), S. 55-64
- /5/ BASSI, A. S.; BRIENS, C. L.; BERGOUGNOU, M. A.: Short Contact Time Fluidized Reactors (SCTFRs), *Proceedings Circulating Fluidized Bed Technology (CFB) IV, 1993, Hidden Valley, Somerset, PA* (1995), S. 15-19
- /6/ TESCH, M.: Zeitkonstantes Dosieren feiner Feststoffe, *Diss. ETH Nr. 9593*, Zürich, 1991
- /7/ MEILI, R.: Kontinuierliche Erzeugung homogener Gas-/Feststoffsuspensionen für effiziente Fallrohrreaktoren, *Diss. ETH Nr. 11199, Fortschr.-Ber. VDI Reihe 3 Nr. 417*, Düsseldorf: VDI Verlag, 1995
- /8/ NICOLAI, R.: Experimentelle Untersuchung zur Strömungsmechanik in einer hochexpandierten Gas/Feststoff-Wirbelschicht, *Diss. ETH Nr. 11344*, Zürich, 1995
- /9/ EMICKE, K.: Flame Cyclone Reactor (FCR), *116th AIME Meeting, Denver* (1987), S. 1-11
- /10/ PUSATERI, J. F.; BOUNDS, C. O.; LHERBIER, L. W.: Zinc Recovery Via the Flame Reactor Process, *Journal of Metals* (1988), S. 31-35
- /11/ Gas-Fired Flame Reactor Technology Enters Commercial Use, *GRID* (1993)
- /12/ BOUNDS, C. O.; PUSATERI, J. F.: EAF Dust Processing in the Gas-Fired Flame Reactor Process, *Lead-Zinc-Tin '90, World Symposium, Anaheim California* (1990)
- /13/ GOEDICKE, F., MEILI, R.: Processing of Fly-Ash Using a Short-Term Conctrolled Feeding System, *12th International Congress of Chemical and Process Engineering (CHISA), Prague/Tschechia, august 1996*
- /14/ KOOPMANN, E. W.; ZUIDEVELD, R. W. Regenbogen P. L.: Erfahrungen mit dem Shell-Kohlevergasungsprozess, *VGB Kraftwerkstechnik* 74 (1994), Nr. 11, S. 974-977
- /15/ SOHN, H. Y.; SEO, K. W.: *Flash Combustion of Sulfide Mineral Particles in a Turbulent Gas Jet/Multiphase Transport and Particle Phenomena*, Bd. 3. Hemisphere Publ. Corp., New York, 1991
- /16/ PUSATERI, J. F.; ZAGROCKI, R. J.: The HRD Reactor Process for Treatment of Contaminated Soils, *Air and Waste Management Asociation* (1992), S. 1-13
- /17/ ROQUES, Y.: Caractérisation Hydrodynamique d'un Réacteur Fluidisé Ultra-Rapidè, *Thèse, Institut Français Du Pétrole (IFP), Université Pierre et Marie Curie* (1994), S. 1-343
- /18/ WIJFFELS, J.-B.: The Shell Coal Gasification Process - Clean Coal Technology for Power Generation with High Efficiency, *Int. Conference on Coal, the Environment and Development: Technologies to Reduce Greehouse Gas Emissions, Proceedings, Sydney* (1991), S. 421-426
- /19/ SCHELLBERG, W.: Combined Cycle (IGCC) with Prenflo and its Contribution to Reducing Greenhouse Gas Emission, *Int. Conference on Coal, the Environment and Development: Technologies to Reduce Greehouse Gas Emissions, Proceedings, Sydney* (1991), S. 427-434
- /20/ SCHELLBERG, W.; WETZEL, R.: Neue Erkenntnisse zur Kohledruckvergasung im Flugstrom, *VGB Kraftwerkstechnik* 70 (1990), Nr. 3, S. 221-225
- /21/ SCHELLBERG, W.: Prenflo-Demonstrations-Anlage in Fürstenhausen - Betriebserfahrungen Kohlevergasung, *BWK* 39 (1987), Nr. 5, S. 238-240
- /22/ CARPENTER, A. M.; SKORUPSKA, N. M.: Coal Combustion - Analysis and Testing, *IEACoal Research, London* 64 (1993), S. 15-46

- /23/ KNILL, K. J.; MAALMAN, T.F.J.; MORGAN, M. E.: Development of a Combustion Characterization Technique for high Volatile Bituminous Coals, *Research Report, IFRF, IJmuiden* IFRF Doc. No. F 88/a/10 (1989)
- /24/ SMART, J. P.: Coal Combustion Research, *Annex II IEA Coal Combustion Sciences, Research Report II, IFRF, IJmuiden*, S. 23-33
- /25/ SAITO, M.; SADAKATA, M.; SATO, M.; SOUTOME, T.; MURATA, H.; OHNO, Y.: Combustion Rates of Pulverized Coal Particles in High-Temperature/High-Oxygen Concentration Atmosphere, *Combustion and Flame* 87 (1991), S. 1-12
- /26/ HAM, A. J.; DER RIET, M. van: Eine genaue Beurteilung des Verbrennungsverhaltens von Kraftwerkskohlen, *VGB Kraftwerkstechnik* 73 (1993), Nr. 4, S. 370-377
- /27/ VAN HEEK, K.-H.; MÜHLEN, H.-J.; RANKE, U.: Einfluss des Sauerstoffpartialdruckes auf die Kinetik der Pyrolyse und Verbrennung von Steinkohlen, *CIT* 65 (1993), Nr. 3, S. 323-327
- /28/ LORSON, H.; SCHINGNITZ, M.: Konversionsverfahren zur thermischen Verwertung von Rest- und Abfallstoffen, *BWK* 46 (1994), Nr. 5, S. 214-217
- /29/ LORSON, H.: Pyrolyse und Druckvergasung von Abfällen, *VGB-Tagungsbericht "Feuerungen 1994"* TB 217 (1994)
- /30/ RAGHUNATHAN, K.; DASTIDAR, A. G.; FAN, L.-S.: High temperature reactor system for study of ultrafast gas-solid reactions, *Rev. Sci. Instrum.* 64 (1993), Nr. 7, S. 1989-1993
- /31/ GULLET, B. K.: Design and characterization of a 1200 °C entrained flow, gas/solid reactor, *Rev. Sci. Instrum.* 59 (1988), Nr. 9, S. 1980-1984
- /32/ BJERLE, I.; XU, F.; YE, Z.: Useful Experimental Technique for the Study of Heterogeneous Reactions, *Chem. Eng. Technol.* 15 (1992), S. 151-161
- /33/ MORGAN, N.: Schwebeschmelzverfahren: Um Längen vor dem Feld, *Finnische Technologie* (1992), S. 20-21
- /34/ DONALDSON, L.: Industrial Glass Process Innovations, *Gas Research Institute*
- /35/ GANS, I.; GAUVIN, W. H.: The Plasma Production of Ultrafine Silica Particles, *The Canadian Journal of Chemical Engineering* 66 (1988), S. 438-444
- /36/ GIACOBBE, F. W.; SCHMERLING, D. W.: Design and Use of an Efficient Plasma Jet Reactor for High Temperature Gas/Solid Reactions, *Mat. Res. Soc. Symp. Proc.* 30 (1984), S. 133-141
- /37/ R. STEVENS: Zirconia and Zirconia Ceramics, *Magnesium Elektron Ltd.*, S. 10,11
- /38/ SEKIGUCHI, H.; HONDA, T.; KANZAWA, A.: Thermal Plasma Decomposition of Chlorofluorocarbons, *Plasma Chemistry and Plasma Processing* 13 (1993), Nr. 3, S. 463-478
- /39/ RUTHNER, M. J.: Microstructure Development of Presintered Ferrite Powders Using a Short Thermal Treatment Within a Vertical Furnace, *Submicronox, CH-6340 Baar*, S. 1-5
- /40/ KUHN, P.: Metal Oxides - Candidates for Solar Energy Conversion,, S. 22-25
- /41/ STEINFELD, A.; IMHOF, A.; MISCHLER, D.: Experimental Investigation of an Atmospheric-Open Cyclone Solar Reactor for Solid-Gas Thermochemical Reactions,, S. 26-29
- /42/ BISWAS, D. R.: Development of novel ceramic processing, *Journal of Materials Science* (1989), Nr. 24, S. 3791-3798
- /43/ POOK, H.; RIZZON, J.: Die Mineralisierung von Klärschlamm nach dem CORMIN-N-Verfahren, *Entsorgungs Praxis-Spezial* (1991), Nr. 3, S. 40-45

- /44/ STRÖMBERG, S.; NURMI, P.; LILIUS, G.; JYRKÖNEN, S.; JOKILAAKSO, A.: Oxidation of Nickel Concentrates and Crushed Nickel Matte, *Extraction & Processing Division (EPD) Congress 1995 in Las Vegas, NV, The Minerals, Metals & Materials Society (TMS)* (1995), S. 207-222
- /45/ JORTIKKA, M.; HELLE, L.; HANNIALA, P.: Improving Copper Smelting Process, Capacity and Costs - The Answer is Outokumpu Flash Smelting, *Extraction & Processing Division (EPD) Congress 1994 in San Francisco, CA, The Minerals, Metals & Materials Society (TMS)* (1994), S. 669-687
- /46/ TAYLOR, P. R.; MANRIQUE, M.; PIRZADA, S. A.: Production of Value-Added Materials by Direct Treatment of Ilmenite Concentrates in a Thermal Plasma Reactor, *Extraction & Processing Division (EPD) Congress 1995 in Las Vegas, NV, The Minerals, Metals & Materials Society (TMS)* (1995), S. 49-59
- /47/ MAKINO, A.; ARAKI, N.; KUWABARA, T.: Flammability Limits, Dilution Limits and Effect of Particle Size on Burning Velocity in Combustion Synthesis of TiC, *JSME, Series B 37* (1994), Nr. 3, S. 576-582